The effect of structural disorder on the secondary electron emission of graphite

L. A. Gonzalez,[1,2] R. Larciprete,[1,3] and R. Cimino[1]
[1]*LNF-INFN, Via E. Fermi 40, 00044 Frascati, Roma, Italy*
[2]*Autonoma University of Madrid, Spain*
[3]*CNR-ISC Istituto dei Sistemi Complessi, Via Fosso del Cavaliere 100, 00133 Roma, Italy*

The dependance of the secondary electron yield (SEY) on the degree of crystallinity of graphite has been investigated during the amorphization of a highly oriented pyrolytic graphite (HOPG) samples by means of Ar^+ bombardment. Photoemission and Raman spectroscopies were used to follow the structural damage while the SEY curves were measured from very low energies up to 1000 eV. We found that the increase of lattice defects lowers the contribution of the π electrons in the valence band and loss spectra and smears out the intense modulations in the low energy secondary electron yield (LE-SEY) curve. Raman spectroscopy results showed that ion induced lattice amorphization is confined in a near-surface layer. The evolution of SEY curves was observed with the progressive Ar^+ dosage after crystal damage as due to the modification of the electronic transport properties within the damaged near surface layer.

The use of graphitic thin films is known to be an efficient solution to mitigate electron cloud (e^-Cloud) phenomena in high energy particle (HEP) accelerators[1–6] due to the low secondary electron yield (SEY) properties of sp^2 carbon. Recently, carbon coatings have been proposed as the base line design of high luminosity large hadron collider (HL-LHC)[7] and potentially, for future circular colliders (FCC-hh).[8] However, such films may lack of structural quality and be additionally damaged once they will be exposed, during machine operation, to electron, photon and, in particular, ion bombardment. It is therefore important to validate the low SEY properties of graphitic films while their structural quality is altered by external factors.[5] In the present study special attention was paid not only to the variation of the maximal SEY value (SEY_{max}) but also to the more subtle changes on the entire SEY curve, with a particular attention to the SEY at low (< 40eV) primary electron energy (LE-SEY),[9] that has been recently shown to play an important role in the e^-Cloud buildup. We introduced controlled amounts of crystal damage in a highly oriented pyrolytic graphite (HOPG) sample by subsequent cycles of Ar^+ ion bombardment at low kinetic energy (500 eV). In the case of graphene, the effect of the impact of the low energy Ar^+ ions has been recently investigated.[10–12] It has been shown that Ar^+ impact determines the intercalation of Ar atoms below graphene after removal of C atoms and that the vacancy dimensions and relative distances grow and decrease, respectively, with increasing irradiation dose. When moving from single layer to bulky graphitic samples, the ion induced damaging extends to deeper layers depending on the ion kinetic energy. Low energy ion bombardment can generate interstitial defects created by trapping incident ions underneath the carbon planes.[13–15]

The structural defects originated in HOPG by the Ar^+ bombardment may have specific effects on both the maximum value and the shape of its SEY curve, specially at very low energies. Such variations are expected as due to changes in the electronic and structural properties of HOPG, which were monitored by in situ ultraviolet (UPS) and X-ray photoelectron spectroscopy (XPS) and ex-situ Raman spectroscopy.

The experiment was performed at the Material Science Laboratory of the INFN-LNF, Frascati (Rome), in an ultra-high vacuum (UHV) system consisting of a preparation chamber and an analysis

chamber, both having a base pressure of $\sim 1 \times 10^{-10}$ mbar. The HOPG sample was cleaved with adhesive tape before being loaded into the UHV system. Prolonged thermal annealing at temperatures of ~1000 K was carried out to desorb contaminants whose absence was then crosschecked by XPS. The HOPG was Ar^+ ion bombarded at 500 eV and Ar pressure of 5×10^{-6} mbar for increasing dose up to $4.5 \times 10^{14} \pm 0.1$ Ar^+/cm^2. TRIM[16] software was used to estimate the penetration depth of 500 eV Ar ions impinging on HOPG. A value of 1.9 ± 0.4 nm was obtained in good agreement with previously published experimental data.[17] After each ion dose, UPS and XPS analysis of the surface, as well as SEY measurements were carried out. Then the HOPG was brought to atmosphere and after Raman analysis procedure, cleaved again and loaded into the UHV system to perform the following Ar^+ dosage cycle. For the UPS and XPS spectra an Omicron EA125 analyzer was used to analyze the photoelectrons excited by the non monochromatic radiation of a HeII (40.8 eV) or a MgKα (1253.6 eV) source respectively. The secondary electron yield is defined as $SEY = I_{out}/I_0 = (I_0 - I_s)/I_0$, being I_0 the current of the primary electron beam impinging onto the sample, as measured by an ad-hoc designed Faraday cup, I_{out} the current of the electrons emerging from the sample and I_s the sample current to ground, as measured by a precision amperometer. The collection efficiency of such measuring systems is taken, as in all relative literature, to be equal to 1. SEY data as a function of the primary energy E_0 are characterized by a maximum value (SEY_{max}) reached in correspondence of a certain energy ($E_{0,m}$). The SEY and LE-SEY ($E_0 < 40\,eV$) measurement technique and its accuracy is described in detail in[1,3,4,9,18]. As already discussed,[9] we can correctly measure SEY starting from few hundreds of meV above the sample work function (WF). In agreement with literature[19] graphite WF was set at 4.83 eV above the Fermi level for all samples studied. Although the graphite work function has been observed to increase by ~0.2 eV[20] after Ar^+ bombardment at ion kinetic energy and dose comparable with ours, we neglected this variation in Fig. 1 The Raman spectra were measured ex-situ by using a Horiba XploRA Raman microscope system with a ×100 objective at $\lambda = 532$ nm. Laser power was kept at 1 mW to avoid heat induced sample damage or graphitization.

Fig. 1 shows the SEY curves measured for increasing Ar^+ dose as a function of the energy of the primary electron beam. The SEY of pristine HOPG exhibits a maximum value of 1.0[1,21,22] in the whole E_0 range between 220 and 400 eV. As the ion dose increases, the SEY progressively decreases for primary energies $E_0 > 200$ eV while SEY_{max} shifts to, $E_{0,m}$, as low as ~175 eV. After $4.5 \times 10^{14} Ar^+/cm^2$ the SEY at 1000 eV reduces from 0.8 measured for the pristine HOPG to 0.6. Also SEY_{max} decreases to 0.95 for low bombarding dose whereas for doses higher than 8.5×10^{13} Ar^+/cm^2, rises to 1.1. This shows that carbon samples going from perfectly crystalline to significantly damaged graphite have, in all studied cases, a favorable low SEY_{max} value. However the

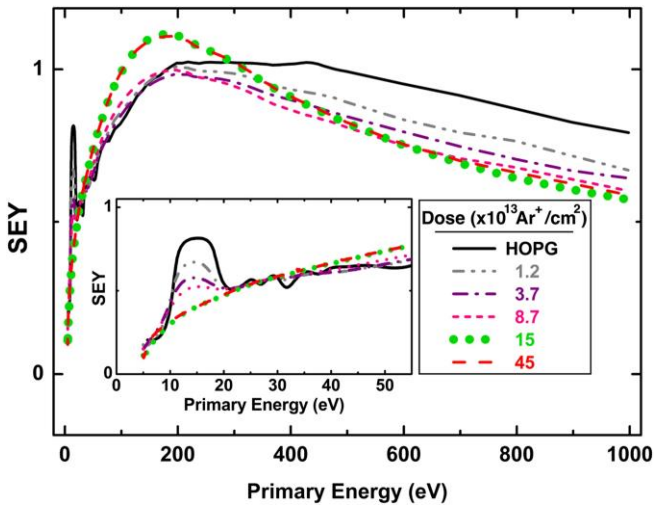

FIG. 1. SEY and LE-SEY (inset) curves measured on HOPG as cleaved (black line) and after the exposure to increasing doses of Ar^+ ions at 500 eV.

effect of the structural quality of the graphitic lattice on more subtle details like LE-SEY behavior or $E_{0,m}$ values, which may be relevant to qualify a surface material in terms of multipacting, requires a more detailed investigation. The LE-SEY curves shown in the inset of Fig. 1, exhibit a nearly total absence of any reflected component. This is in agreement with previously published results,[9] suggesting that the absence of a significant low energy reflected component is a strong signature a of clean conducting surface. Moreover, it has been proved that such behavior is independent of the degree of crystallinity of the measured sample. Then, as the primary energy rises, the SEY gradually increases. For energies $E_0 > 5$ eV above the Fermi level, the curve of pristine HOPG shows structures related to the elastic and inelastic electron-solid interactions, providing direct information on the unoccupied band structure of graphite.[23,24] It is clearly observable how the spectral structures of LE-SEY are progressively smeared out as ion dose increases. At doses of 1.5×10^{14} Ar^+/cm^2, the curve reaches a smooth profile remaining stable after further Ar^+ doses.

The extent of Ar^+ induced HOPG amorphization was monitored by UPS spectroscopy of the valence band measured at normal emission. Fig. 2a shows the spectrum of the intact HOPG exhibiting sharp features at 4.3 (σ band) and 7.5 eV (π band).[25] The peak just above the Fermi Level is related to photoelectron emission excited by the He II satellite (hv = 48.4 eV). Both bands decrease in intensity already at 1.2×10^{13} Ar^+/cm^2 which parallels the evolution of the LE-SEY spectral structures. The presence of broad unstructured features observed for doses higher than 5.0×10^{13} Ar^+/cm^2 indicates a total amorphization of the crystalline structure. Fig. 2b shows the XPS C1s spectra measured on HOPG before Ar^+ bombardment and after the highest dose. For the pristine sample the peak is located at BE of 284.15 eV, typical for sp^2 hybridized C atoms. After the Ar^+ dose, the C1s peak remains centered at the same BE confirming that the C atom hybridization is not affected by ion bombardment, since typically the sp^3 and sp^2 fingerprint components are found with a separation of 0.8-0.9 eV.[1] The increase of the C1s FWHM from 0.7 eV to 1.1 eV is attributed to the presence of defects in the crystalline network. It should be noted that the HOPG line shape, which typically has a FWHM of 0.3 eV[26] is broadened by the limited energy resolution (~0.7 eV) of our experimental setup. Ar signal was below the detection limit of XPS analysis. This suggests that the grazing impact geometry used in this experiment reduces the Ar trapping probability enhancing its desorption and self-sputtering.[27] Fig. 2c also shows the corresponding energy loss spectra produced by inelastically scattered C1s core level electrons. Two features are observed at 6 and 30 eV above the C1s peak maximum corresponding to the carbon π and π + σ plasmons respectively. After ion bombardment, the π plasmon signal smears out in agreement with crystal amorphization. The extinction of the π plasmon has been attributed[28] to the creation of interstitial defects, responsible of increasing the interplanar spacing between the carbon planes, which diminish both the semimetallic character and the conductivity of graphite.

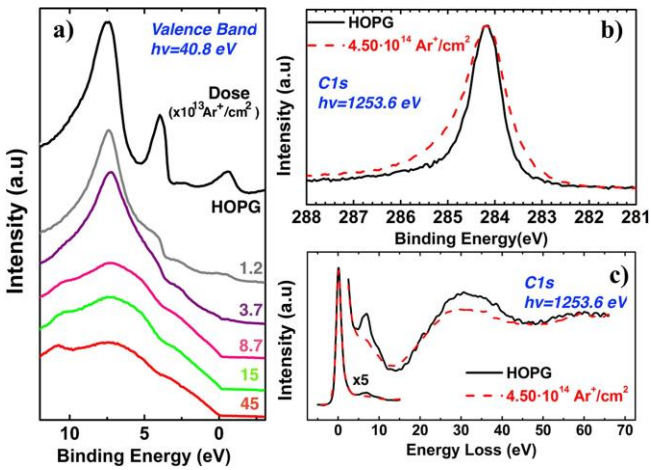

FIG. 2. a: Valence band spectra measured on the pristine HOPG sample and after the exposure to increasing dose of Ar^+ ions at 500 eV. b: C1s core level and c: energy loss spectra measured before Ar^+ bombardment and after the highest dose.

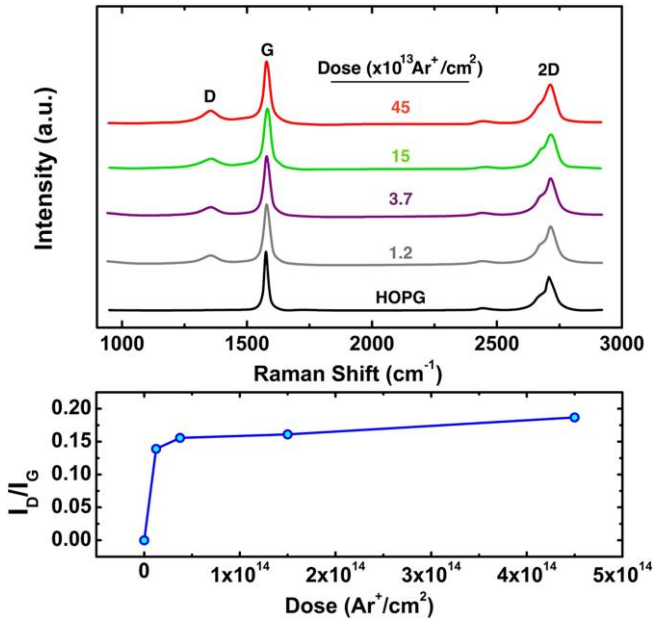

FIG. 3. Top: Raman spectra taken on the HOPG sample before ion bombardment and after the exposure to increasing Ar^+ dose. Bottom: D/G Raman peaks ratio vs Ar^+ dose.

Fig. 3 shows Raman spectra measured on HOPG as a function of the ion dose. For pristine HOPG the spectrum is composed of two bands, G at 1585 cm^{-1} that arises from the vibrations of the sp^2 bonds and 2D, that is the second order of the D peak and appears at 2700 cm^{-1}. After ion bombardment, with the onset of lattice disorder, the peak D, which is prohibited in perfect hexagonal lattice, appears at 1350 cm^{-1}, as the presence of defects in the aromatic rings makes it allowed.[29] The ratio R=D/G is plotted in Fig. 2b. It can be observed that R reaches an almost complete saturation after an Ar^+ dose of 3.7×10^{13} Ar^+/cm^2. The observed evolution of R is in good agreement with previous experimental findings[30] and indicates that, according to the estimated ion penetration depth (~1.9 nm), ion induced damaging is confined in a thin sample layer smaller than the Raman sampling depth (~ 500 nm).[31] Our studied sample can in fact be schematically considered as a bi-layer structure formed by a bulk crystalline HOPG with an increasingly amorphized (with bombardment) carbon layer of fixed thickness at the surface.

In order to rationalize the SEY curves shown in Fig. 1 it should be considered that the secondary electron emission properties can be strongly dependent on the material surface morphology and roughness.[4] Atomic force microscopy was used to state that the effect of highest Ar^+ sputtering dose was only to slightly increase the roughness value from 0.5 nm measured on the intact surface to less than 0.7 nm. Such a limited change in surface roughness strongly suggests that its role in the SEY evolution can be confidently neglected. Another possible factor causing a SEY variation is a change in the sample work function. It is known that the work function of graphite exposed to the Ar^+ ion doses used in this study increases by ~0.2 eV.[20] Such a variation may result in a SEY decrease in the whole E_0 range, being higher the barrier that secondary electrons have to overcome to escape from the sample. Conversely, the curves shown in Fig. 1 with the SEY decreasing only for E_0 higher that 300 eV indicate that the mechanism regulating the electron emission is more complex. In order to explain the SEY behavior observed in Fig. 1 it should be kept in mind that, according to previous experimental findings,[32–35] the localized states that appear near the defect sites act as scattering centers for electron waves, which play an important role in the transport properties[36] of the damaged HOPG surface layer. Such phenomena are then expected to have significant effect on SEY and its LE part[37,38] within the region affected by the bombardment. In fact, considering the bi-layered structure of the bombarded sample, its transport properties must depend on whether the electrons move through the damaged overlayer or through the underlying pristine HOPG. The penetration depths of 200 eV and 1000 eV impinging electrons, which for intact graphite are ~2 nm and ~30 nm,

respectively[39] are consistently reduced in the presence of scattering defects. Therefore, in the ion bombarded sample, 200 eV primary electrons cannot cross the damaged region, whose thickness has been estimated by TRIM to be 1.9 nm, and extinguish in a thinner near-surface layer. Then, even if for secondary electrons the IMFP is lower than in intact graphite (~0.4 nm at their typical kinetic energy of 50 eV)[40] the curves of Fig. 1 show that at $E_0 \sim 200$ eV the overall effect of charge scattering at lattice defects is a SEY increase. On the other hand, electrons impign with $E_0 \sim 1000$ eV will certainly cross the damaged layer and generate secondary electrons within the undamaged underlying HOPG. In this case, even if the penetration depth is lower than in intact graphite, the reduction in mobility and IMFP that secondary electron suffer when traveling towards the surface through the defected graphite lattice reduces their effective number emerging from the sample. This effect explains the gradual SEY depletion at high E_0 values (see Fig. 1) with increasing ion dose and crystalline disorder in the C layer. The data presented here may trigger specific calculations, helping to reach a quantitative understanding of the effect of disorder and induced defects on transport and IMFP properties of carbon compounds.

In conclusion, here we show the importance of studying the stability and aging of carbon based coatings during particle accelerator operation. Amorphization of HOPG has been proved to be capable of modifying sample SEY curve. Nevertheless SEY_{max} values remained relatively stable and low (<1.1) even after amorphization, which confirms sp^2 hybridization as a must for carbon coatings regarding the mitigation of e^-Cloud effects. Clearly, when more subtle details (like $E_{0,m}$ or LE-SEY behavior) are relevant to the qualification of a surface as an e^-Cloud mitigator, its detailed crystalline quality may play a role and must be studied in details. It is shown here that the absence of any reflected component observed in the LE-SEY data, typical of clean conductors, is actually independent of the graphite crystalline quality. Moreover, LE-SEY spectra were shown to strongly depend not only on the chemistry of the coating but also on the density of lattice defects, which may have significant implications on simulations where SEY and LE-SEY curves are parametrized.

ACKNOWLEDGMENTS

The authors wish to thank A. Di Gaspare for the atomic force microscopy measurements. This work was supported by INFN Group V IMCA project. We acknowledge the staff of DAΦNE-Light for technical assistance, and the Spanish National Plan of I+D+i Coordinated Projects No. AYA2012-39832-C02- 01.

[1] R. Cimino, M. Commisso, D. R. Grosso, T. Demma, V. Baglin, R. Flammini, and R. Larciprete, Phys. Rev. Lett. **109**, 064801 (2012).
[2] C. G. H. Walker, M. M. El-Gomati, A. M. D. Assa'd, and M. Zadražil, Scanning **30**, 365 (2008).
[3] R. Larciprete, D. Grosso, M. Commisso, R. Flammini, and R. Cimino, Phys. Rev. ST Accel. Beams **16**, 011002 (2013).
[4] R. Cimino and T. Demma, Int. J. Mod. Phys. A **29**, 1430023 (2014).
[5] R. Larciprete, D. R. Grosso, A. Di Trolio, and R. Cimino, Appl. Surf. Sci. **328**, 356 (2015).
[6] C. Y. Vallgren, G. Arduini, J. Bauche, S. Calatroni, P. Chiggiato, K. Cornelis, P. C. Pinto, B. Henrist, E. Mètral, H. Neupert, G. Rumolo, E. Shaposhnikova, and M. Taborelli, Phys. Rev. ST Accel. Beams **14**, 071001 (2011).
[7] G. Apollinari, CERN Yellow Reports **5**, 1 (2016).
[8] R. Cimino, V. Baglin, and F. Schäfers, Phys. Rev. Lett. **115**, 264804 (2015).
[9] R. Cimino, L. Gonzalez, R. Larciprete, A. Di Gaspare, G. Iadarola, and G. Rumolo, Phys. Rev. ST Accel. Beams **18**, 051002 (2015).
[10] E. H. Ahlgren, S. K. Hämäläinen, O. Lehtinen, P. Liljeroth, and J. Kotakoski, Phys. Rev. B **88**, 155419 (2013).
[11] G. Zamborlini, M. Imam, L. L. Patera, T. O. Menteş, N. Stojić, C. Africh, A. Sala, N. Binggeli, G. Comelli, and A. Locatelli, Nano Lett. **15**, 6162 (2015).
[12] R. Larciprete, S. Colonna, F. Ronci, R. Flammini, P. Lacovig, N. Apostol, A. Politano, P. Feulner, D. Menzel, and S. Lizzit, Nano Lett. **16**, 1808 (2016).
[13] J. R. Hahn and H. Kang, Physical Review B **60**, 6007 (1999).
[14] D. Marton, H. Bu, K. J. Boyd, S. S. Todorov, A. H. Al-Bayati, and J. W. Rabalais, Surf. Sci. **326**, L489 (1995).
[15] J. R. Hahn, H. Kang, S. Song, and I. C. Jeon, Phys. Rev. B **53**, R1725 (1996).
[16] J. F. Ziegler, M. D. Ziegler, and J. P. Biersack, Nucl. Instrum. Methods B **268**, 1818 (2010).
[17] T. Li, B. V. King, R. J. MacDonald, G. F. Cotterill, D. J. O'connor, and Q. Yang, Surf. Sci. **312**, 399 (1994).
[18] R. Cimino, I. R. Collins, M. A. Furman, M. Pivi, F. Ruggiero, G. Rumolo, and F. Zimmermann, Phys. Rev. Lett. **93**, 014801 (2004).
[19] S. Mathur, Proc. Phys. Soc. **50**, 495 (1952).
[20] H. Hashimoto, M. Watanabe, S. Nishiuma, K. Nakamura, and S. Yoshida, Surf. Inetrface Anal. **35**, 19 (2003).
[21] N. R. Whetten, J. Appl. Phys. **34**, 771 (1963).
[22] J. M. Ripalda, I. Montero, L. Vázquez, D. Raboso, and L. Galán, J. Appl. Phys. **99**, 043513 (2006).

[23] P. J. Mølert and M. H. Mohamed, J. Phys. C: Solid State Phys. **15**, 6457 (1982).
[24] R. F. Willis, B. Fitton, and G. S. Painter, Phys. Rev. B **9**, 1926 (1974).
[25] S. Y. Zhou, G.-H. Gweon, C. D. Spataru, J. Graf, D.-H. Lee, S. G. Louie, and A. Lanzara, Phys. Rev. B **71**, 161403 (2005).
[26] F. Sette, G. K. Wertheim, Y. Ma, G. Meigs, S. Modesti, and C. T. Chen, Phys. Rev. B **41**, 9766 (1990).
[27] W. Choi, C. Kim, and H. Kang, Surf. Sci. **281**, 323 (1993).
[28] M. Portail, J. B. Faure, T. Angot, and J. M. Layet, Surf. Sci. **581**, 24 (2005).
[29] A. C. Ferrari and J. Robertson, Phys. Rev. B **61**, 14095 (2000).
[30] A. Jorio, M. M. Lucchese, F. Stavale, E. H. M. Ferreira, M. V. Moutinho, R. B. Capaz, and C. A. Achete, J. Phys.: Condens. Matter **22**, 334204 (2010).
[31] Z. Ni, Y. Wang, T. Yu, and Z. Shen, Nano Res. **1**, 273 (2010).
[32] T. Tanabe, Phys. Scr. **1996**, 7.
[33] N. Gorjizadeh, A. A. Farajian, and Y. Kawazoe, Nanotechnology **20**, 015201 (2009).
[34] D. L. Maslov, V. I. Yudson, A. M. Somoza, and M. Ortuño, Phys. Rev. Lett. **102**, 216601 (2009).
[35] F. Banhart, ACS Nano **5**, 26 (2010).
[36] A. Lherbier, B. Biel, Y. M. Niquet, and S. Roche, Phys. Rev. Lett. **100**, 036803 (2008).
[37] G. F. Dionne, J. Appl. Phys. **44**, 5361 (1973).
[38] G. F. Dionne, J. Appl. Phys. **46**, 3347 (1978).
[39] K. Kanaya and S. Okayama, J. Phys. D: Appl. Phys **5**, 43 (1972).
[40] S. Tanuma, C. J. Powell, and D. R. Penn, Surf. Interface Anal. **43**, 689 (2011).